THE JOURNAL OF BIOLOGICAL CHEMISTRY VOL. 286, NO. 48, pp. 41616–41625, December 2, 2011

Structural and Evolutionary Basis for the Dual Substrate Selectivity of Human KDM4 Histone Demethylase Family*[S]

Received for publication, July 18, 2011, and in revised form, September 9, 2011 Published, JBC Papers in Press, September 13, 2011, DOI 10.1074/jbc.M111.283689

Lars Hillringhaus[‡1], Wyatt W. Yue[§], Nathan R. Rose[‡], Stanley S. Ng[§], Carina Gileadi[§], Christoph Loenarz[‡], Simon H. Bello[‡], James E. Bray[§], Christopher J. Schofield[‡2], and Udo Oppermann[§¶3]

From the [‡]Department of Chemistry and the Oxford Centre for Integrative Systems Biology, Chemistry Research Laboratory, University of Oxford, 12 Mansfield Road, Oxford, OX1 3TA, the [§]Structural Genomics Consortium, University of Oxford, Old Road Campus Roosevelt Drive, Headington, OX3 7DQ, and the [¶]Botnar Research Centre, National Institute for Health Research Oxford Biomedical Research Unit, Nuffield Department of Orthopedics, Rheumatology, and Musculoskeletal Sciences, Oxford, OX3 7LD, United Kingdom

Background: Lysine demethylases reverse N^{ϵ}-methylation in a sequence- and methylation-selective manner.
Results: Enzyme-histone interactions away from the conserved oxygenase active site are important in determining sequence selectivity in the JMJD2 (KDM4) subfamily.
Conclusion: The catalytic JmjC domain determines sequence selectivity for at least some JmjC demethylases.
Significance: This work might be a basis for the development of selective inhibitors.

N^{ϵ}-Methylations of histone lysine residues play critical roles in cell biology by "marking" chromatin for transcriptional activation or repression. Lysine demethylases reverse N^{ϵ}-methylation in a sequence- and methylation-selective manner. The determinants of sequence selectivity for histone demethylases have been unclear. The human JMJD2 (KDM4) H3K9 and H3K36 demethylases can be divided into members that act on both H3K9 and H3K36 and H3K9 alone. Kinetic, crystallographic, and mutagenetic studies *in vitro* and in cells on KDM4A–E reveal that selectivity is determined by multiple interactions within the catalytic domain but outside the active site. Structurally informed phylogenetic analyses reveal that KDM4A–C orthologues exist in all genome-sequenced vertebrates with earlier animals containing only a single KDM4 enzyme. KDM4D orthologues only exist in eutherians (placental mammals) where they are conserved, including proposed substrate sequence-determining residues. The results will be useful for the identification of inhibitors for specific histone demethylases.

Multiple modifications to histones collectively enable transcriptional regulation and play critical roles in DNA replication and repair (1). Lysines are probably the most extensively modified histone residues, undergoing N^{ϵ}-mono/di/tri-methylation, acetylation, as well as ubiquitination and other modifications. Once thought to be irreversible, histone lysine methylation is now recognized as a dynamic process (2). Two families of histone-lysine demethylases (KDM enzymes (3)) have been identified as follows: the flavin-dependent lysine-specific demethylases (KDM1 (3, 4)) and the larger Fe(II)-dependent Jumonji C (JmjC) family, which employ 2-oxoglutarate (2OG)[4] and oxygen as cosubstrates (5, 6). The JmjC demethylases are linked to diseases, including cancer (*e.g.* through involvement of KDM2B (7), FBXL (10), KDM4A/B/C (JMJD2A/B/C) (8), and KDM5B (JARID1B) (9, 10)) and mental retardation (*e.g.* KDM5C (JARID1C) (11–16) and PHF8 (17–23)). Distinct JmjC demethylase subfamilies with different sequence and "methylation state" selectivities have been identified (supplemental Fig. 1) (5, 24). With respect to sequence selectivity, some JmjC demethylases are apparently specific for a single methylation site (*e.g.* KDM5A–D for H3K4), whereas others can demethylate at two (*e.g.* KDM4A–C) or more (*e.g.* PHF8) methylation sites. Crystal structures have provided insights into JmjC structures and suggest that methylation state selectivity may be primarily determined by the active site topology (25–29). However, there is a poor understanding of how sequence selectivity is achieved. In at least one case, PHF8, the binding of a noncatalytic plant homeobox domain (PHD) to a modified lysine is important in guiding another particular methylated lysine to a JmjC domain for demethylation (17, 27, 30). In other cases, the available evidence is that sequence selectivity is determined, at least in part, by binding to the "catalytic" 2OG oxygenase domain.

There are six members (*KDM4A–F*) of the human *KDM4* (*JMJD2*) subfamily, of which two, *KDM4E/F*, are likely to be pseudogenes (31). KDM4A and -C are the best studied members of the KDM4 subfamily and have roles in development,

* This work was supported in part by the Biotechnology and Biological Sciences Research Council, the Wellcome Trust, and by the Oxford National Institute for Health Research Oxford Biomedical Research Biomedical Research Unit.
⌘ *Author's Choice*—Final version full access.
[S] The on-line version of this article (available at http://www.jbc.org) contains supplemental Figs. 1–8, Tables 1 and 2, and additional references.
The atomic coordinates and structure factors (codes 2XML and 2W2I) have been deposited in the Protein Data Bank, Research Collaboratory for Structural Bioinformatics, Rutgers University, New Brunswick, NJ (http://www.rcsb.org/).
[1] Recipient of a postdoctoral fellowship from the German Academic Exchange Service.
[2] To whom correspondence may be addressed. Tel.: 44-1865-275625; Fax: 44-1865-275674; E-mail: christopher.schofield@chem.ox.ac.uk.
[3] To whom correspondence may be addressed. Tel.: 44-1865-617585; Fax: 44-1865-737231; E-mail: udo.oppermann@sgc.ox.ac.uk.

[4] The abbreviations used are: 2OG, 2-oxoglutarate; PDB, Protein Data Bank; Bistris propane, 1,3-bis[tris(hydroxymethyl)methylamino]propane; Jmj, Jumonji.

cancer, and stem cell biology (8, 32–35). KDM4A/B/C catalyze demethylation of tri- and di-methylated forms of both histone H3 lysine 9 (H3K9me3/me2) and lysine 36 (H3K36me3/me2) (8, 32, 36–39). However, KDM4D and KDM4E (which is catalytically active) only catalyze demethylation of H3K9me3/me2 (37, 38, 40, 41).

Here, we report combined structural, biochemical, and cellular studies on the determinants that regulate sequence selectivity within the KDM4 demethylase subfamily. The results reveal that binding interactions away from the conserved oxygenase active site are important in determining selectivity and that the sequence-determining residues are conserved among eutherian KDM4Ds.

EXPERIMENTAL PROCEDURES

Assays—Peptides were synthesized using a CS-Bio automated solid-phase peptide synthesizer as reported previously (26). The catalytic domains of human KDM4A–E were produced as N-terminally His-tagged proteins in *Escherichia coli* and purified by nickel affinity chromatography as reported previously (26). Variants were generated using the QuikChange™ and QuikChange™ multisite site-directed mutagenesis kit (Stratagene), and mutations were confirmed by DNA sequencing. Purified enzymes were incubated with Fe(II), 2OG, ascorbate, and peptide and analyzed by MALDI-TOF mass spectrometry as reported previously (42). Kinetic constants were determined using a formaldehyde dehydrogenase-coupled assay as reported previously (41). For the competition assays, equal concentrations (10 μM) of the respective peptides were used. Aliquots were taken from the reaction mixture at specific time points, quenched with MeOH (1:1), and analyzed by MALDI-TOF MS. Demethylation assays using bulk calf thymus type II-A histones (Sigma H9250) using Western blot analysis was performed as reported previously (17). Immunofluorescence assays were performed as reported previously (43).

Crystallization and Structure Determination of KDM4C and KDM4E—Crystals of KDM4C were grown at 4 °C by vapor diffusion in sitting drops mixing protein (7 mg/ml with 2 mM *N*-oxalylglycine) and well solution (25% (v/v) PEG3350, 0.2 M sodium nitrate, 0.1 M Bistris propane, pH 6.5, 5% (v/v) ethylene glycol, 0.01 M $NiCl_2$) in a 2:1 ratio. Crystals were cryo-protected using 25% (v/v) ethylene glycol and flash-cooled in liquid nitrogen. Diffraction data extending to 2.55 Å resolution were collected at the Diamond Light Source beamline I24. Crystals of KDM4E were grown at 4 °C by vapor diffusion in sitting drops mixing protein (10 mg/ml with 2.5 mM 2,4-pyridinedicarboxylic acid) and well solution (20% (v/v) PEG3350, 0.1 M sodium citrate, pH 5.5, 2 mM $NiCl_2$) in a 2:1 ratio. Crystals were cryo-protected using 25% (v/v) glycerol and flash-cooled in liquid nitrogen. Diffraction data extending to 2.1 Å resolution were collected at the Swiss Light Source beamline X10SA. Diffraction data were processed using the CCP4 program suite (44). The structures of KDM4C and KDM4E were determined by molecular replacement using the program PHASER (45) with the human KDM4A structure (PDB code 2OQ7) as a search model. Automated model building was performed with ARP/wARP (46), followed by iterative cycles of restrained refinement and model building using REFMAC (47) and COOT (48). All residues are within the favored and allowed regions of the Ramachandran plot.

Bioinformatic Analyses—KDM4 orthologues were identified by BLAST searches in eukaryotic genome databases from NCBI (http://www.ncbi.nlm.nih.gov), Ensembl, and JGI (http://www.jgi.doe.gov). A multiple sequence alignment of the JmjN and JmjC domains of KDM4 orthologues from different organisms was carried out using ClustalW2 and refined using GeneDoc. A phylogenetic tree was generated from the aligned sequences and visualized using TraceSuite II. Protein domains were identified using the SMART and Pfam databases.

Accession Codes—Coordinates for KDM4C and KDM4E have been deposited under the accession codes 2XML and 2W2I, respectively, in the Protein Data Bank.

RESULTS

Kinetic Analyses of the Human KDM4 Family—To investigate the determinants of sequence selectivity within the KDM4 subfamily, we initially produced the catalytic domains of human KDM4A–E in recombinant form (KDM4F is very similar to KDM4E sharing 94% identity over 369 residues) and assayed them for activity by MS using 12–15-residue peptide fragments of histone H3. The results support previous reports (8, 32, 36, 38–40) that all the KDM4 members demethylate the tri- and di-methylated N^{ϵ}-methylated forms (demethylation of H3K9me3 to H3K9me0 was observed on prolonged incubation of 15-residue H3K9me3 peptides) and that KDM4A/B/C act on both H3K9 and, less efficiently, on H3K36-methylated substrates (Fig. 1*A*). In contrast, KDM4D and -E only act on H3K9, with no evidence for demethylation of H3K36, even after prolonged incubations. Competition experiments, in which we used a 1:1 ratio of H3K9me3 and H3K36me3 peptides, demonstrate that each of KDM4A/B/C preferentially catalyze demethylation at Lys-9 rather than Lys-36 under identical conditions (Fig. 1*B*). Competition experiments employing H3K9me3 (which contained ^{13}C-labeled glycine residues to distinguish the demethylated products in mass spectrometric analysis from those resulting from H3K9me2 demethylation) and H3K9me2 also revealed a clear preference for the tri- over the di-methylated state for all the five analyzed KDM4 members (Fig. 1*C*).

We then investigated kinetic parameters for the KDM4 isoforms for both tri- and di-methylation states using an eight-residue H3K9 sequence. We were unable to obtain reliable kinetic parameters for the H3K36 substrates because of the relatively low levels of activity at this site. For all KDM4 members, the K_m values for H3K9me3 were similar or slightly lower than for H3K9me2 (Table 1). The k_{cat} values for the KDM4A/B/C enzymes were higher for H3K9me3 compared with H3K9me2 but very similar for both methylation states for KDM4D and -E. Thus, for the expressed enzymes KDM4A–E, the increased relative efficiency for demethylation of the tri-methylated state correlates with differences in both K_m and k_{cat} values, with differences in K_m and k_{cat} alone being relatively more important for KDM4D and KMD4E, respectively.

Overall, the kinetic analyses clearly revealed that KDM4A/B/C accepted both H3K9 and H3K36 as substrates, whereas KDM4D/E only accepted H3K9. The combined K_m and k_{cat} values for the H3K9 substrates suggest that differences in rates

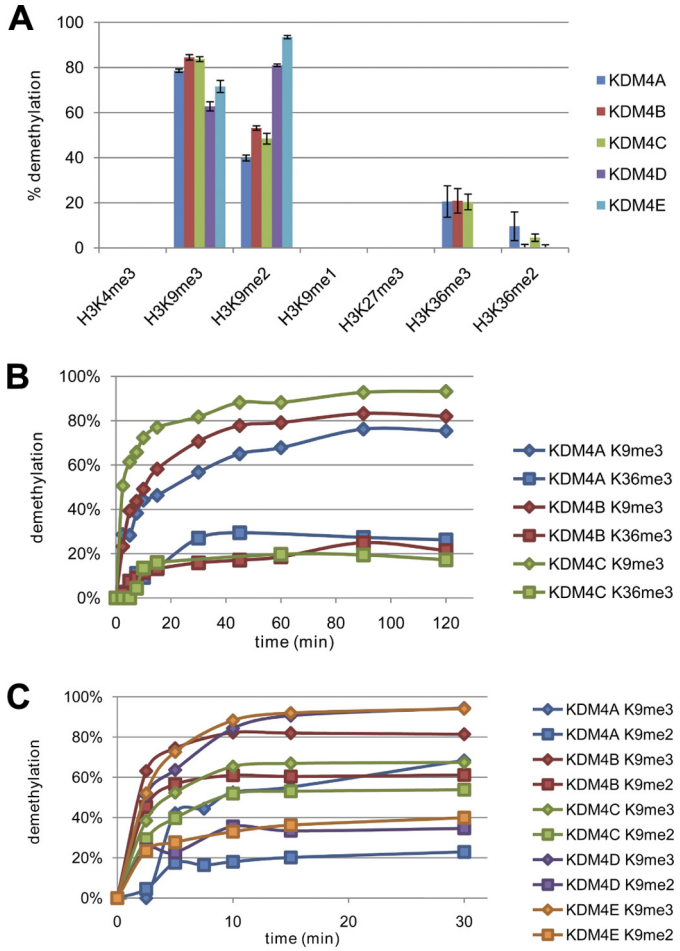

FIGURE 1. **Substrate selectivity of the human KDM4 histone demethylase subfamily.** *A,* results using $H3_{1-9}$K4me3, $H3_{1-15}$K9me3, $H3_{1-15}$K9me2, $H3_{1-15}$K9me1, $H3_{24-33}$K27me3, $H3_{30-41}$K36me3, and $H3_{30-41}$K36me2 as substrates. The extent of demethylation was measured after a 30-min incubation (37 °C). *B,* results of competition assay between $H3_{6-17}$K9me3 and $H3_{30-41}$K36me3. *C,* results of competition assays between $H3_{1-15}$K9me3[^{13}C]G12-[^{13}C]G13 and $H3_{1-15}$K9me2 peptides. Pairs of competing peptides are *color-coded*. In each case, incubations (37 °C) were analyzed by MS after quenching with MeOH (1:1). *Errors* represent S.D. of three replicates.

of demethylation, and hence selectivity, may arise both from differences in substrate binding and rate of reaction once bound as enzyme-substrate complexes. We then investigated how differences in substrate-binding interactions lead to differences in sequence selectivity by carrying out crystallographic analyses on the two different subgroups of KDM4 enzymes.

Structural Basis of Sequence Selectivity between KDM4 Members—In addition to the described structures for KDM4A (26) and KDM4D (PDB code 3DXU), we determined the structure of KDM4C in complex with Ni^{2+} and *N*-oxalylglycine at 2.55 Å resolution and the structure of KDM4E in complex with Ni^{2+} and the KDM4 inhibitor 2,4-pyridinedicarboxylic acid (41) at 2.10 Å resolution (supplemental Table 1 and Fig. 3). The overall architectures of the catalytic domains of KDM4C and KDM4E are highly similar to other members of the KDM4 family (supplemental Table 2 and Fig. 3 and Fig. 2), with only minor structural differences observed (*e.g.* the zinc-binding site is disordered in KDM4E, likely as a result of the crystallization conditions). The structures also share a closely related active site topology with respect to metal and 2OG binding; nickel (substituting iron) ion is coordinated by the conserved HX(E/D) . . . H motif and in a bidentate manner by a close 2OG analogue (*N*-oxalylglycine in KDM4C and 2,4-pyridinedicarboxylic acid in KDM4E).

To investigate the underlying structural features resulting in differences in substrate selectivity between the KDM4A/B/C and KDM4D/E subgroups, we inspected the residues lining the active site and the substrate binding region (Fig. 3). Consistent with the kinetic analyses demonstrating a general preference of the tri- and di- over the mono-methylated states, all KDM4 subfamily members have highly conserved residues lining the methylammonium-binding pocket. The exceptions are Ser-288_A/Ser-289_B/Ser-290_C and Thr-289_A/Thr-290_B/Thr-291_C in KDM4A, -B, and -C (the KDM isoform is denoted by a subscript), which are substituted by Ala-287_D/Ala-289_E/Ala-286_F and Ile-288_D/Ile-290_E/Ile-287_F in KDM4D–F, respectively (the structures of KDM4B and -F were modeled based on the other structures). Chen *et al.* (38) have reported that the KDM4A S288A/T289I double variants show high activity for both H3K9me3/me2 and H3K36me/me2. We thus proposed that interactions responsible for the sequence selectivity are likely outside the methylammonium-binding pocket and focused on identifying such potential interactions.

Comparison of the KDM4A-H3K9 and -H3K36 substrate structures with the KDM4E structure reveals surface differences in the peptide-binding site that we considered may underlie the lack of activity toward H3K36 substrates for KDM4D/E (Fig. 3). Importantly, all differences in peptide-enzyme interactions, as described below for KDM4A *versus* KDM4E, are conserved within the KDM4A–C and KDM4D/E subgroups (Fig. 3*A*), thus allowing us to analyze substrate specificity for the KDM4D/E sub-branch using KDM4E as a model system. Besides its N^{ϵ}-methyl lysine interactions, in KDM4A, the H3K36 peptide, which adopts a bent conformation centered around Pro-38_{H3}, is apparently bound by interactions, including those involving Thr-32_{H3}, Gly-33_{H3}, Val-35_{H3}, Lys-37_{H3}, and Tyr-41_{H3}. Thr-32_{H3}-Oγ is positioned to hydrogen bond to the Ser-316_A backbone amide, which is conserved among all KDM4 members (Fig. 3*A*). The main-chain amide and/or carbonyl groups of Gly-33_{H3}, Val-35_{H3}, Lys-37_{H3}, and Tyr-41_{H3} are positioned to form hydrogen bonds with the backbone amide and/or carbonyl groups of Lys-314_A, Asp-311_A, Ala-69_A and Asn-86_A, respectively. These residues are conserved among KDM4A–C and substituted by Thr-318_D/Thr-315_E, Ala-315_D/Ser-312_E, Thr-73_D/Thr-70_E, and His-90_D/His-87_E in KDM4D/E, respectively. However, the analogous KDM4D/E residues are unlikely to enable H3K36 activity because the enzyme-substrate interactions mediated by them apparently only involve backbone interactions. We therefore considered other interactions involved in H3K36 binding, including those not immediately apparent from the crystal structures.

Analysis of the KDM4A H3K36me3 structure suggests that a negatively charged surface is involved in binding the positively charged side chains of Lys-37_{H3} and, possibly, Arg-40_{H3} (Fig. 3), for the side chains of His-39_{H3} and Arg-40_{H3}, electron density was not observed. The region possibly contributing to Arg-40_{H3} binding is altered in KDM4E compared with KDM4A;

TABLE 1

Kinetic analyses of the KDM4 subfamily

Kinetic analysis of the methylation state selectivity for the KDM4 subfamily members with $H3_{7-14}$K9me3 and H37–14K9me2 employing an HCHO release assay. Errors represent S.D. of three replicates.

KDM	$H3_{7-14}$K9me2			$H3_{7-14}$K9me3		
	K_m	k_{cat}	k_{cat}/K_m	K_m	k_{cat}	k_{cat}/K_m
	μM	s^{-1}	$s^{-1}\ \mu M^{-1} \times 10^4$	μM	s^{-1}	$s^{-1}\ \mu M^{-1} \times 10^4$
KDM4A	73 ± 26	0.0029 ± 0.0004	0.4	45 ± 7	0.010 ± 0.0005	2.2
KDM4B	50 ± 11	0.0050 ± 0.0004	1.0	31 ± 10	0.028 ± 0.002	9.0
KDM4C	66 ± 14	0.0072 ± 0.0005	1.1	48 ± 9	0.029 ± 0.002	6.0
KDM4D	74 ± 6	0.012 ± 0.0003	1.6	37 ± 9	0.015 ± 0.001	4.1
KDM4E	25 ± 3	0.065 ± 0.002	26.0	23 ± 4	0.076 ± 0.01	33.0

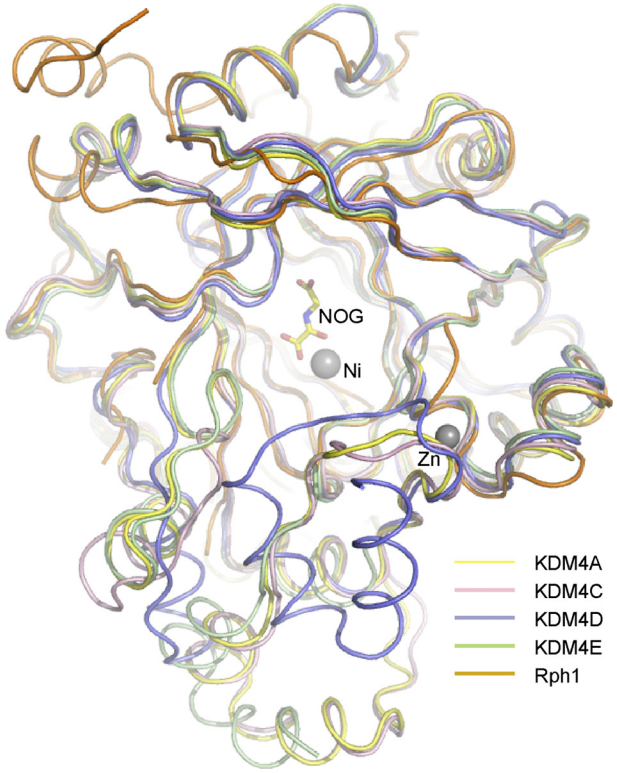

FIGURE 2. **Comparison of the Zn(II)-binding sites of human and yeast KDM4 members as observed in crystal structures for KDM4A,C,D,E and Rph1.** Note that in case of the KDM4D structure (*blue*, PDB code 3DXU) there are substantial differences in secondary structure affecting parts of the Zn(II) (*dark sphere*) binding loop. The zinc-binding site in KDM4E is disordered possibly due to loss of zinc in the crystallization process. NOG, *N*-oxalylglycine.

Gln-88_A is substituted by Lys-89_E likely causing a consequent alteration in electrostatic properties. Further differences in KDM4A/KDM4E substrate binding may occur at residues Leu-72_E, His-87_E, and Lys-88_E in KDM4E (Ile-71_A, Asn-86_A, and Ile-87_A in KDM4A), two of which might decrease H3K36 binding by increasing positive charge. In KDM4A, Tyr-41-Oγ_{H3} is within hydrogen-bonding distance of the terminal nitrogens of the guanidino group of Arg-309_A (Fig. 3), which is located in a loop forming part of the zinc-binding site of the KDM4 family. In KDM4E, the corresponding segment is disordered (possibly due to loss of zinc during crystallization); however, sequence comparisons reveal that the homologous residue to Arg-309_A is Gly-310_E, which would not be able to form the H-bonding contacts to Tyr-41-Oγ_{H3} observed in KDM4A. Overall, these analyses suggest that Ile-71_A, Asn-86_A, Ile-87_A, Gln-88_A, and Arg-309_A are involved in the productive binding of the H3K36 substrate in KDM4A–C.

Further structural analyses suggested that Ile-71_A, Asn-86_A, Ile-87_A, Gln-88_A, and Arg-309_A may not be required for binding of H3K9 substrate. The H3K9me3 peptide is, besides interactions in the methylammonium-binding pocket, bound by residues Asn-86_A, Asp-135_A, Glu-169_A, Tyr-175_A, and Lys-241_A which, except for Asn-86_A, are conserved among all KDM4 members (Fig. 3*A*). In the KDM4A-H3K9me3 structure, Asn-86_A is positioned to form two hydrogen bonds with the main-chain carbonyl of Gly-13_{H3}. In KDM4D/E Asn-86_A, which is conserved in KDM4B/C, is replaced by His-90_D and His-87_E. Based on a comparison of the KDM4A H3K9me3 substrate structure (PDB code 2OQ6) with KDM4E (PDB code 2W2I), we proposed that His-90_D and His-87_E are also capable of hydrogen bonding with the main-chain carbonyl of Gly-13_{H3} of H3K9me3 consistent with the observation that both KDM4A and -E accept H3K9 substrates. We therefore proposed Ile-71_A, Asn-86_A, Ile-87_A, Gln-88_A, and Arg-309_A as important potential determinants of the H3K9/H3K36 sequence selectivities between KDM4A and KDM4E.

Generation of Variants with Altered Sequence Selectivity—We then tested the structurally based predictions on selectivity by mutagenesis studies. We generated KDM4A variants for each of the residues, which we predicted to determine sequence selectivity in KDM4E (I71L, N86H, I87K, Q88K, and R309G) and analyzed their ability to demethylate peptides with different methylation states at H3K9 and H3K36. The I71L, Q88K, and a quintuple variant, in which all five residues were substituted, demethylated H3K9me3 to H3K9me2 and H3K9me1 in a similar manner to wild-type KDM4A under standard conditions (Fig. 4*A*). The other variants were less active with the H3K9me3 substrate. For the H3K9me2 substrate only the Q88K variant showed the same extent of demethylation compared with wild-type KDM4A, whereas the other variants showed ~50% less demethylation compared with wild-type KDM4A; moreover, no demethylation of H3K9me2 was observed for the R309G variant. None of the variants, except Q88K, demethylated the H3K36me3 and H3K36me2 substrates after 1 h. However, after a 5-h incubation the I71L and R309G variants catalyzed ~5–10% demethylation of H3K36me3, respectively.

Because the endogenous substrates of histone demethylases are histones, we aimed to exclude the possibility that the altered specificity of the KDM4A variants was only observed due to the relatively short substrate length of peptides compared with full-length histones. Therefore, we incubated the variants, wild-type KDM4A and -E, with bulk histones. Analysis by Western blotting using antibodies against H3K9me3 and K36me3

A

	H3Thr32	H3Gly33	H3Val35	H3Lys37	H3Arg40				H3Tyr41
KDM4A	Ser316	Lys314	Asp311	Ala69	(Ile71)	(Ile87)	(Gln88)	Asn86	Arg309
KDM4B	Ser317	Lys315	Asp312	Ala70	(Ile72)	(Ile88)	(Gln89)	Asn87	Arg310
KDM4C	Ser318	Lys316	Asp313	Ala71	(Ile73)	(Ile89)	(Gln90)	Asn88	Arg311
KDM4D	Ser320	Thr318	Ala315	Thr73	(Leu75)	(Lys91)	(Lys92)	His90	Gly313
KDM4E	Ser317	Thr315	Ser312	Thr70	(Leu72)	(Lys88)	(Lys89)	His87	Gly310

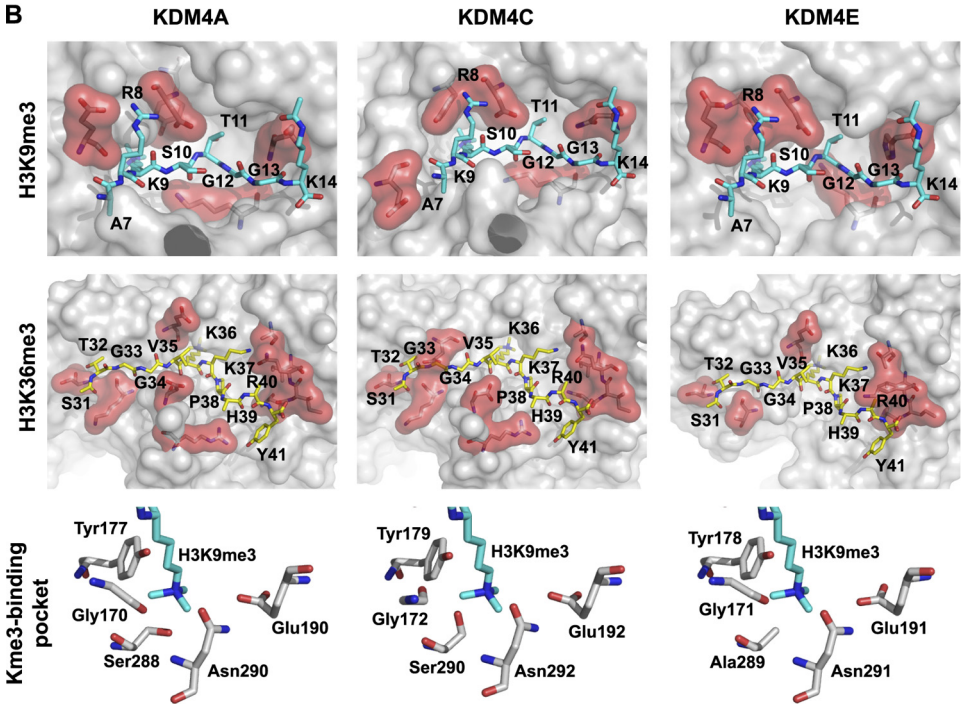

FIGURE 3. **Structural comparisons of the KDM4 subfamily reveal potential determinants of sequence selectivity.** *A,* residue differences between KDM4D/E (*dark gray*) and KDM4A/B/C (*light gray*) subgroups in the H3K36 peptide binding region as observed in KDM4A-substrate crystal structures. Proposed interactions in *brackets* were not observed in these crystal structures likely due to missing electron density for the Arg-40$_{H3}$ side chain. *B,* comparison of proposed substrate binding interactions as observed in KDM4A (PDB code 2OS2), KDM4C (PDB code 2XML), and KDM4E (PDB code 2W2I) structures. KDM4A/C/E are in *gray*, H3K9me3 in *turquoise*, and H3K36me3 in *yellow*. The predicted substrate binding surfaces are in *red*. For KDM4C/E the substrate conformations observed in KDM4A were docked into the active sites.

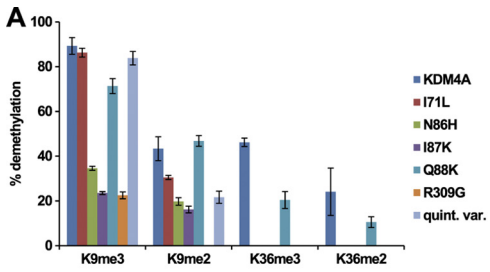

B

KDM	$H3_{7-14}$K9me3		
	k_{cat} (s^{-1})	K_m (μM)	k_{cat}/K_m
KDM4A	0.010 ± 0.0005	45 ± 7	2.3
KDM4A quint. var.	0.004 ± 0.0003	63 ± 13	0.6
KDM4E	0.076 ± 0.001	23 ± 4	33.0

C

KDM	$H3_{7-14}$K9me2		
	k_{cat} (s^{-1})	K_m (μM)	k_{cat}/K_m
KDM4A	0.0029 ± 0.0004	72 ± 26	0.4
KDM4A quint. var.	0.0009 ± 0.0001	5 ± 2	1.8
KDM4E	0.065 ± 0.002	25 ± 3	26.0

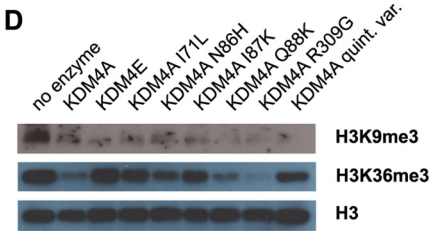

FIGURE 4. **Demethylation of histones by wild type KDM4A and variants.** *A,* demethylation of $H3_{1-15}$K9me3, $H3_{1-15}$K9me2, $H3_{30-41}$K36me3, and $H3_{30-41}$K36me2 by wild type KDM4A and variants. Reactions were at 37 °C and quenched by MeOH (1:1) after 60 min. The amount of demethylation was measured by MS. Errors represent S.D. of three replicates. *B* and *C,* kinetic analysis of the KDM4A quintuple variant with $H3_{7-14}$K9me3 and $H3_{7-14}$K9me2 employing a HCHO release assay. Errors represent S.D. of three replicates. *D,* demethylation of bulk histones by KDM4A variants. Reactions were at 37 °C and quenched by addition of Laemmli buffer after 5 h. KDM4A quintuple variant (*quint. var.*) = I71L, N86H, I87K, Q88K, and R309G.

showed that although all variants demethylated H3K9me3, only the Q88K and R309G variants demethylated H3K36me3, consistent with the results with H3K9/K36 fragments (Fig. 4*D*).

We then evaluated the specificity of the KDM4A variants in cells. A construct encoding for FLAG-tagged KDM4A was subjected to site-directed mutagenesis to generate the I71L and

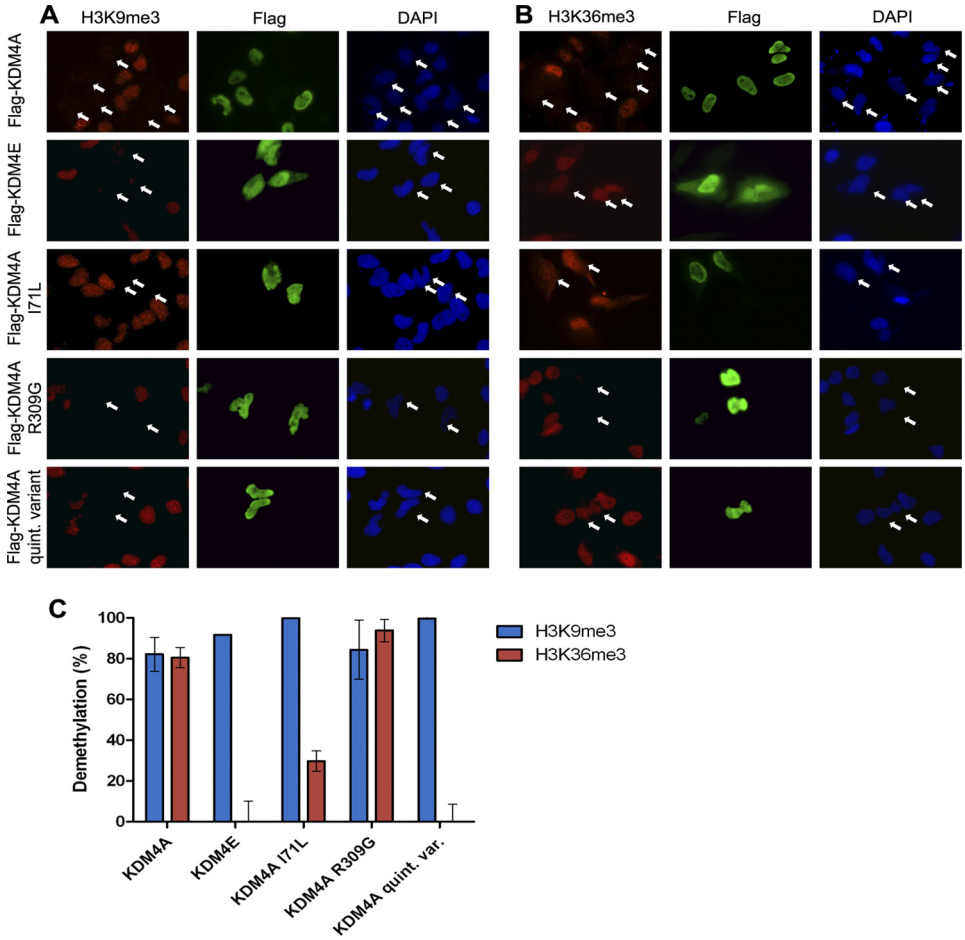

FIGURE 5. **Demethylation of H3K9me3 and H3K36me3 in human cells.** Wild type KDM4E, KDM4A, and variants were expressed in HeLa cells as FLAG fusion proteins. Immunofluorescence assays with antibodies against methylated histone (*left panels*) or FLAG (*middle panels*) were used to analyze the activity of the proteins. DAPI (4,6-diamidino-2-phenylindole) staining (*right panels*) indicates location of nuclei. *A* and *C*, overexpression of KDM4A, KDM4E, and the I71L, R309G, and quintuple KDM4A variant enzymes led to a substantial loss of H3K9me3. *B* and *C*, KDM4A wild type and the KDM4A R309G variant showed a substantial loss of H3K36me3; the KDM4A I71L variant showed slightly reduced H3K36me3 levels; KDM4E and the KDM4A quintuple variants (*quint. var.*) do not reduce H3K36me3 levels. *Errors* represent S.D. of three replicates.

quintuple variants, *i.e.* those that were the most effective variants *in vitro* in demethylating H3K9 but not H3K36. The R309G variant was generated as a control. KDM4A, KDM4E, and the KDM4A variants were overexpressed in HeLa cells, and the levels of methylated lysines were analyzed by indirect immunofluorescence staining using antibodies against H3K9me3 and H3K36me3. For all the enzymes, a substantial loss (80%) of the H3K9me3 level was observed (Fig. 5, *A* and *B*). However, although overexpression of the wild-type KDM4A and R309G variant also resulted in a substantial reduction of K36me3 levels, overexpression of the quintuple variant and, to a lesser extent, the I71L variant did not reduce the H3K36me3 levels, in agreement with the results with purified recombinant enzymes.

Phylogenetic Analysis of KDM4 Demethylases—Using structurally informed cross-genomic bioinformatic analysis, we then sought to investigate the conservation of selectivity determinants in KDM4 subfamily members in eukaryotes for which genome sequences are available. The results reveal that at least one KDM4 orthologue exists in all analyzed eukaryotes ranging from humans to *Trichoplax adherens* (the simplest known animal), choanoflagellates (*Monosiga brevicollis*), and yeasts (Fig. 6). All orthologues are predicted to contain a catalytic JmjC domain with the double-stranded β-helix fold and conserved Fe(II)- and 2-OG-binding residues typical of 2OG oxygenases as well as the Zn(II)-binding motif characteristic of the catalytic domain of the KDM4 family and a JmjN domain (which is known to be required for catalytic activity (36)); hence, they are likely to have demethylase activity (supplemental Fig. 4). The identified vertebrate and most invertebrate KDM4 enzymes contain dual PHD and Tudor domains (Fig. 6 and supplemental Figs. 5 and 6), implying conserved functional roles for the non-catalytic domains. Notably, the analyses further reveal that single orthologues of each of human KDM4A/B/C exist in all analyzed vertebrates, in support of experimental data in human, mice (33, 49–52), and chicken (35) suggesting that they have biologically nonredundant and important roles. Zebrafish contains one additional KDM4 protein likely resulting from the fish-specific genome duplication in the teleost fish lineage (53); the additional zebrafish orthologue has different residue features than all analyzed KDM4Ds, and phylogenetic analysis suggests that it has evolved away from KDM4A–D (supplemental Figs. 7 and 8). Significantly, in addition to KDM4A–C, KDM4D orthologues only exist in eutherians (placental mammals) where they are conserved; although all the identified

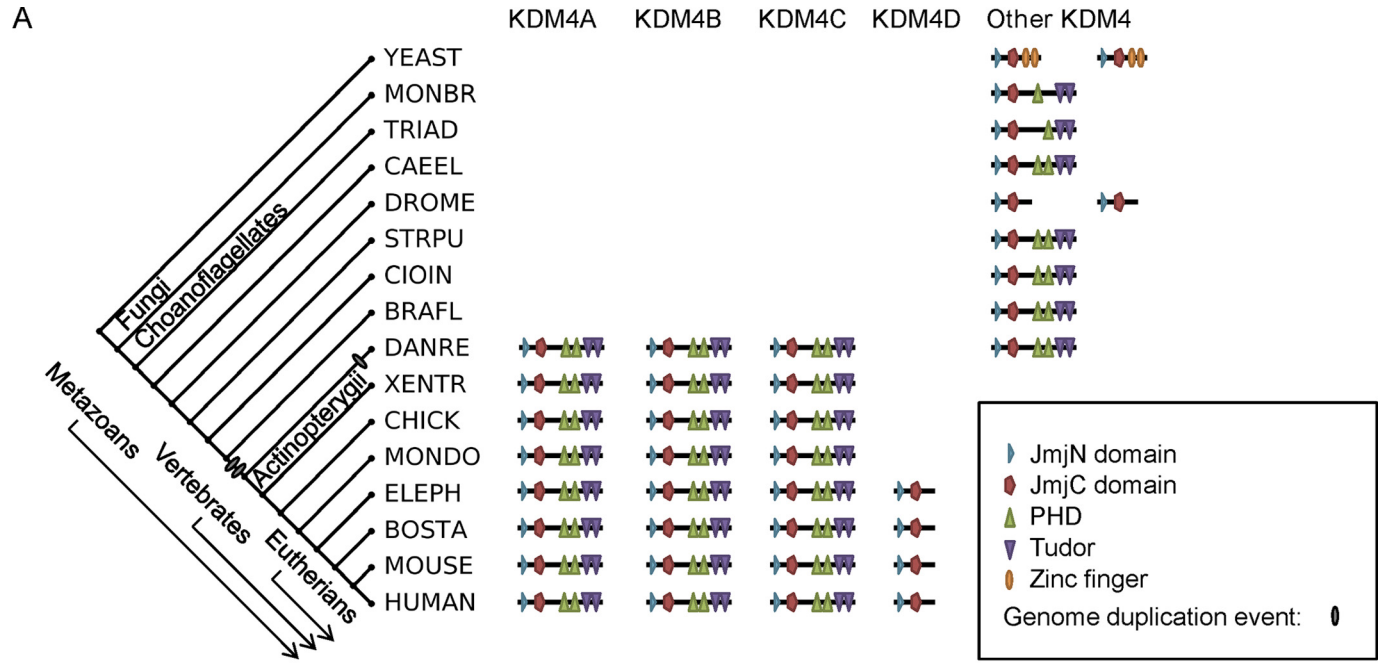

B

```
humanKDM4D   1 : METMKSKANCAQNPNCNIMIFHPTKEEFNDFDKYIAYMESQGAHRAGLAKIIPPKEWKARETYDNISEILIATPLQQVASGRAGVFTQYHKKKKAMTVGEYRHLAN : 106
mouseKDM4D   1 : ---MKTKSTCAQNPNCSIMIFRPTKEEFNDFDKYIAYMESQGAHRAGLAKVIPPKEWRARQSYDNISNILIATPLQQVVSGQAGVFTQYHKKKKGMTVGEYRELAN : 103
bostaKDM4D   1 : --MEAMKPSCAQNPSCSIMIFHPTKEEFTDFDKYIAYIESQGAHRAGLAKIVPPKEWKARQTYDDINDILITAPLQQVVSGRAGVFTQYHKKKKAMTVAEYRHLAN : 104
elephKDM4D   1 : ---MKSKVSCAQNPTCSIMIFHPTKEEFNNFDKYIAYMESQGAHRAGLAKIIPPKEWKARETYDDVNDILIATPLQQVVSGRAGVFTQYHKKKKAMTVGEYRHLAD : 103

humanKDM4D 107 : SKKYQTPPHQNFEDLERKYWKNRIYNSPIYGADISGSLFDENTKQWNLGHLGTIQDLLEKECGVVIEGVNTPYLYFGMWKTTFAWHTEDMDLYSINYLHLGEPKTW : 212
mouseKDM4D 104 : SKKYQTPPHLDFEDLERKYWKNRLYESPIYGADVSGSLFDGKTQQWNVGHLGTIQDLLEQECGIVIEGVNTPYLYFGMWKTTFAWHTEDMDLYSINYLHFGQPKTW : 209
bostaKDM4D 105 : TEKYQTPFYSDFEELERKYWKTRLFESPIYGADISGSLFDENTKQWNLGRLGTIQDLLEQECGVVIEGVNTPYLYFGMWKTAFAWHTEDMDLYSINFLHFGEPKTW : 210
elephKDM4D 104 : SDKYRTPPHLDFEDLERKYWKNRLYDSPIYGADISGSLFDGNTEHWNLGNLGTIQDLLEQECGVVIEGVNTPYLYFGMWKTTFAWHTEDMDLYSINYLHFGEPKTW : 209

humanKDM4D 213 : YVVPPEHGQRLERLARELFPGSSRGCGAFLRHKVALISPTVLKENGIPFNRITQEAGEFMVTFPYGYHAGFNHGFNCAEAINFATPRWIDYGKMASQCSCGEARVT : 318
mouseKDM4D 210 : YAVPPEHGRRLERLARELFPGSSQGCQAFLRHKVALISPTVLKENGIPFCRITQEAGEFMVTFPYGYHAGFNHGFNCAEAINFATPRWIDYGKVASQCSCGEARVS : 315
bostaKDM4D 211 : YAVPPEHGRRLERLAGALFPGSSRSCEAFLRHKAALISPTVLRDNGIPFCRVTQEAGEFMVTFPYGYHSGFNHGFNCAEAINFATPRWIDYGKVASQCSCGEAQVA : 316
elephKDM4D 210 : YAVPPEHGRRLERLARELFPGSARGCEAFLRHKVALISPTVLRENGIPFSRITQEAGEFMVTFPYGYHAGFNHGFNCAEAINFATPRWVDYGKVASQCSCGEARVT : 315
```

FIGURE 6. **Evolutionary analysis of the KDM4 demethylase subfamily.** *A,* phylogenetic domain analysis of eukaryotic KDM4 orthologues. Some orthologues in invertebrates lack the PHD and Tudor domains found in vertebrates. The yeast orthologues Rph1 and Gis1 carry two C-terminal zinc fingers and lack the PHD and Tudor domains. *Ovals* represent genome duplications. Branch lengths and domain sizes are not to scale. Likely pseudogenes (*e.g.* KDM4E/F in humans) are not shown. Note that the JmjC domain of the KDM4 enzymes itself contains a Zn(II)-binding motif. *B,* sequence alignment of eutherian KDM4D orthologues. Fe(II)-binding residues are in *red* and 2OG-binding residues in *blue*. Residues proposed to determine sequence specificity for H3K9 are in *green* and conserved in all analyzed eutherians. *JmjN,* Jumonji N; *JmjC,* Jumonji C; PHD, plant homeobox domain; Tudor, Tudor domain; *bosta*, *Bos taurus*; *eleph*, *Loxodonta africana*; *mondo*, *Monodelphis domestica*; *chick*, *Gallus gallus*; *xentr*, *Xenopus tropicalis*; *danre*, *Danio rerio*; *brafl*, *Branchiostoma floridae*; *cioin*, *Ciona intestinalis*; *strpu*, *Strongylocentrotus purpuratus*; *drome*, *Drosophila melanogaster*; *caeel*, *Caenorhabditis elegans*; *triad, Trichoplax adherens; monbr*, *Monosiga brevicollis*.

KDM4D orthologues contain a single predicted JmjN domain to the N terminus of the JmjC domain, they lack the dual PHD and Tudor domains characteristic of KDM4A–C.

Sequence alignment of KDM4 orthologues from different organisms reveals that the five residues we propose to abolish demethylation of H3K36 (Leu-75$_D$, His-90$_D$, Lys-91$_D$, Lys-92$_D$, and Gly-313$_D$ in human KDM4D) are totally conserved among KDM4Ds from human, mouse, cow, and elephant, implying that the sequence specificity for H3K9 observed for human KDM4D is maintained and that a KDM4D type activity is important in eutherian biology.

Interestingly, the yeast KDM4 orthologue Rph1, which has been shown to demethylate H3K9 and H3K36 *in vitro* and in mammalian cells (54), differs in three of the five selectivity-determining residues from human KDM4A–D (Val-90$_{Rph1}$, Glu-91$_{Rph1}$, and Ile-359$_{Rph1}$ corresponding to Ile-87$_A$, Gln-88$_A$ Arg-309$_A$, Lys-91$_D$, Lys-92$_D$, and Gly-313$_D$ in human KDM4A and KDM4D, respectively) (supplemental Fig. 8). The other two residues Ile-74$_{Rph1}$ and Asn-89$_{Rph1}$ in Rph1 differ from the homologous residues (Leu-75$_D$ and His-90$_D$) in human KDM4D but not from the homologous residues (Ile-71$_A$ and Asn-86$_A$) in human KDM4A (which are conserved among all analyzed KDM4A/B/C) supporting the results of our mutagenesis studies that these residues (in particular Ile-71$_A$, Ile-72$_B$, Ile-73$_C$, and Ile-74$_{Rph1}$) are involved in the dual sequence selectivity of human KDM4A/B/C and yeast Rph1 for H3K9 and H3K36. The differences between Rph1 and KDM4A–C may be responsible for the capability of Rph1 to demethylate H3K9me3 and H3K36me3 with similar efficiencies (54), in contrast to KDM4A/B/C, which preferentially demethylate H3K9me3 over H3K36me3. However, in the reported crystal structure of Rph1 (without substrate, PDB code 3OPT, supplemental Fig. 4*E*) residues which, based on comparison with the KDM4A substrate structure, are likely to be involved in binding of

H3K36me3 are partially missing due to use of a C-terminally truncated construct. Thus, structurally based predictions on how increased activity for H3K36 is achieved by Rph1 are not presently possible.

DISCUSSION

The combined experimental results presented here and elsewhere (8, 32, 36, 37, 40, 49) and phylogenetic analyses on KDM4A–E clearly show that they can be divided into two subclasses, KDM4A–C, which are highly conserved in all vertebrates, and demethylate both H3K9 and H3K36 and KDM4D/E, which only accept H3K9 substrates. KDM4A–C have conserved dual PHD and Tudor domains in addition to their JmjC domains, which are likely involved in "targeting" the catalytic domains (as precedented with PHF8 (30)). The histone marks that are recognized by the Tudor and PHD domains are uncharacterized except for the JMJD2A Tudor domain, which is selective for H3K4me3 and H4K20me3 (55, 56). However, KDM4D–E do not possess such "additional" domains (Fig. 6); thus, it seems likely that at least some of the selectivity of the KDM4 subfamily residues arises from residues in or close to the catalytic domain. Selectivity arising from the catalytic domain may be relatively more important for those members (*e.g.* KDM4D/E) that do not contain additional domains. The altered selectivity features of the generated KDM4A variants reveal that sequence specificity within the KMD4 subfamily is not achieved by differences in the methylammonium-binding pocket but by other enzyme-histone interactions. The dramatic decrease in activity toward H3K36 of the I71L variant and the complete loss for the N86H and I87H variants reveal that these residues are key determinants of the sequence specificity for H3K36. Because the Q88K and R309G variants still demethylated H3K36, including with bulk histones and in cells, these residues are not a major determinant for sequence specificity. Interestingly, the I71L variant showed the same extent of demethylation of H3K9 as wild-type KDM4A. Thus, the interaction between Ile-71 and the H3K36 substrate could be a promising target for sequence-specific inhibitors, which would only inhibit either Lys-9- or Lys-36-directed activity of KDM4A.

The yeast KDM4 orthologue Rph1 has been reported to demethylate both H3K9 and H3K36 *in vitro* and in mammalian cells (54). However, as yet there is no reported methyltransferase acting on H3K9 in budding yeast, and this mark is therefore probably unmethylated. The capacity of Rph1 to demethylate H3K9 was suggested to be a vestige of an H3K9 methylation system in budding yeast. Interestingly, human KDM4A–C have been reported to demethylate non-histone substrates *in vitro* (57, 58), and the identified substrates share sequence similarity to H3K9; the biological significance of these observations is unknown. Thus, we speculate that the activity of Rph1 for H3K9 may result from its putative activity for non-histone substrates in budding yeast or earlier organisms.

The roles of bivalent N^{ϵ}-lysine methylations in transcriptional activation and repression are established for H3K4me3 (activation) and H3K27me3 (repression) for several genes involved in development (59, 60). Related roles are emerging for H3K9me3 and H3K36me3 (35); H3K36me3 accumulates in the 3′-region of active genes, whereas H3K9me3 has been found in the promoter region of repressed genes, as well as in the coding region of active genes (1). The demethylation of H3K9me3/H3K36me3 by KDM4A is proposed to repress transcription (36, 37). However, a recent report implies that KDM4A activates genes in neural crest development by demethylating H3K9me3 at the *Sox10* gene locus; no H3K36me3 was observed at the 3′-end of the *Sox10* gene during active transcription (35). Overall, these and other results imply that the interplay between different methylation states is complex and context-dependent. In this regard, the finding that the sequence selectivity (*i.e.* Lys-9 *versus* Lys-36) can be altered by mutagenesis may also be useful in dissecting the roles of the KDM4 subfamily members and the relative importance of binding and catalytic domains in determining *in vivo* selectivity.

Although the activity toward H3K9 decreased for most point substitutions, replacement of all five residues (I71L, N86H, I87K, Q88K, and R309G) resulted in a variant with similar activity toward H3K9 compared with wild-type KDM4A, implying that there is a synergistic effect between the substitutions and hence binding interactions. Although it cannot be ruled out that *in vitro* studies of JmjC histone demethylases have consistently failed to identify additional stimulatory factors (*e.g.* protein complex partners/other conditions for optimal activity), turnover numbers for the KDM4s are low compared with some other human 2-OG oxygenases, *e.g.* γ-butyrobetaine hydroxylase (61), and comparable with those reported for the hypoxia-inducible factor hydroxylases (62). Given the central role proposed for the hypoxia-inducible factor hydroxylases in regulating the hypoxic response in all animals (63, 64), it is possible that the demethylase activities of the KDM4 histone demethylases have roles in directly regulating gene expression, perhaps in a redox-regulated manner. In this regard, it is interesting that expression of KDM4B is itself regulated in a hypoxia-inducible factor- and hypoxia-dependent manner (65–68), suggesting multiple ways in which oxygen levels regulate histone methylation.

Acknowledgments—The Structural Genomics Consortium is a registered charity (Number 1097737) funded by the Canadian Institutes for Health Research, the Canadian Foundation for Innovation, Genome Canada through the Ontario Genomics Institute, GlaxoSmithKline, Karolinska Institutet, the Knut and Alice Wallenberg Foundation, the Ontario Innovation Trust, the Ontario Ministry for Research and Innovation, Merck, the Novartis Research Foundation, the Swedish Agency for Innovation Systems, the Swedish Foundation for Strategic Research, and the Wellcome Trust. We thank Rob Klose and Yi Zhang for the kind gift of KDM4A and KDM4E plasmid constructs and Xuan Shirley Li, Alexander Wolf, Linda O'Flaherty, Michael A. McDonough, Akane Kawamura and Oliver King for helpful discussions.

REFERENCES

1. Kouzarides, T. (2007) *Cell* **128,** 693–705
2. Shi, Y., and Whetstine, J. R. (2007) *Mol. Cell* **25**, 1–14
3. Allis, C. D., Berger, S. L., Cote, J., Dent, S., Jenuwien, T., Kouzarides, T., Pillus, L., Reinberg, D., Shi, Y., Shiekhattar, R., Shilatifard, A., Workman, J., and Zhang, Y. (2007) *Cell* **131,** 633–636
4. Shi, Y., Lan, F., Matson, C., Mulligan, P., Whetstine, J. R., Cole, P. A., Casero, R. A., and Shi, Y. (2004) *Cell* **119,** 941–953

5. Klose, R. J., Kallin, E. M., and Zhang, Y. (2006) *Nat. Rev. Genet.* **7,** 715–727
6. Tsukada, Y., Fang, J., Erdjument-Bromage, H., Warren, M. E., Borchers, C. H., Tempst, P., and Zhang, Y. (2006) *Nature* **439,** 811–816
7. Pfau, R., Tzatsos, A., Kampranis, S. C., Serebrennikova, O. B., Bear, S. E., and Tsichlis, P. N. (2008) *Proc. Natl. Acad. Sci. U.S.A.* **105,** 1907–1912
8. Cloos, P. A., Christensen, J., Agger, K., Maiolica, A., Rappsilber, J., Antal, T., Hansen, K. H., and Helin, K. (2006) *Nature* **442,** 307–311
9. Yamane, K., Tateishi, K., Klose, R. J., Fang, J., Fabrizio, L. A., Erdjument-Bromage, H., Taylor-Papadimitriou, J., Tempst, P., and Zhang, Y. (2007) *Mol. Cell* **25,** 801–812
10. Xiang, Y., Zhu, Z., Han, G., Ye, X., Xu, B., Peng, Z., Ma, Y., Yu, Y., Lin, H., Chen, A. P., and Chen, C. D. (2007) *Proc. Natl. Acad. Sci. U.S.A.* **104,** 19226–19231
11. Iwase, S., Lan, F., Bayliss, P., de la Torre-Ubieta, L., Huarte, M., Qi, H. H., Whetstine, J. R., Bonni, A., Roberts, T. M., and Shi, Y. (2007) *Cell* **128,** 1077–1088
12. Abidi, F. E., Holloway, L., Moore, C. A., Weaver, D. D., Simensen, R. J., Stevenson, R. E., Rogers, R. C., and Schwartz, C. E. (2008) *J. Med. Genet.* **45,** 787–793
13. Jensen, L. R., Amende, M., Gurok, U., Moser, B., Gimmel, V., Tzschach, A., Janecke, A. R., Tariverdian, G., Chelly, J., Fryns, J. P., Van Esch, H., Kleefstra, T., Hamel, B., Moraine, C., Gecz, J., Turner, G., Reinhardt, R., Kalscheuer, V. M., Ropers, H. H., and Lenzner, S. (2005) *Am. J. Hum. Genet.* **76,** 227–236
14. Santos, C., Rodriguez-Revenga, L., Madrigal, I., Badenas, C., Pineda, M., and Milà, M. (2006) *Eur. J. Hum. Genet.* **14,** 583–586
15. Tzschach, A., Lenzner, S., Moser, B., Reinhardt, R., Chelly, J., Fryns, J. P., Kleefstra, T., Raynaud, M., Turner, G., Ropers, H. H., Kuss, A., and Jensen, L. R. (2006) *Hum. Mutat.* **27,** 389
16. Adegbola, A., Gao, H., Sommer, S., and Browning, M. (2008) *Am. J. Med. Genet.* **146A,** 505–511
17. Loenarz, C., Ge, W., Coleman, M. L., Rose, N. R., Cooper, C. D., Klose, R. J., Ratcliffe, P. J., and Schofield, C. J. (2010) *Hum. Mol. Genet.* **19,** 217–222
18. Liu, W., Tanasa, B., Tyurina, O. V., Zhou, T. Y., Gassmann, R., Liu, W. T., Ohgi, K. A., Benner, C., Garcia-Bassets, I., Aggarwal, A. K., Desai, A., Dorrestein, P. C., Glass, C. K., and Rosenfeld, M. G. (2010) *Nature* **466,** 508–512
19. Koivisto, A. M., Ala-Mello, S., Lemmelä, S., Komu, H. A., Rautio, J., and Järvelä, I. (2007) *Clin. Genet.* **72,** 145–149
20. Laumonnier, F., Holbert, S., Ronce, N., Faravelli, F., Lenzner, S., Schwartz, C. E., Lespinasse, J., Van Esch, H., Lacombe, D., Goizet, C., Phan-Dinh Tuy, F., van Bokhoven, H., Fryns, J. P., Chelly, J., Ropers, H. H., Moraine, C., Hamel, B. C., and Briault, S. (2005) *J. Med. Genet.* **42,** 780–786
21. Kleine-Kohlbrecher, D., Christensen, J., Vandamme, J., Abarrategui, I., Bak, M., Tommerup, N., Shi, X., Gozani, O., Rappsilber, J., Salcini, A. E., and Helin, K. (2010) *Mol. Cell* **38,** 165–178
22. Feng, W., Yonezawa, M., Ye, J., Jenuwein, T., and Grummt, I. (2010) *Nat. Struct. Mol. Biol.* **17,** 445–450
23. Fortschegger, K., de Graaf, P., Outchkourov, N. S., van Schaik, F. M., Timmers, H. T., and Shiekhattar, R. (2010) *Mol. Cell. Biol.* **30,** 3286–3298
24. Klose, R. J., and Zhang, Y. (2007) *Nat. Rev. Mol. Cell Biol.* **8,** 307–318
25. Couture, J. F., Collazo, E., Ortiz-Tello, P. A., Brunzelle, J. S., and Trievel, R. C. (2007) *Nat. Struct. Mol. Biol.* **14,** 689–695
26. Ng, S. S., Kavanagh, K. L., McDonough, M. A., Butler, D., Pilka, E. S., Lienard, B. M., Bray, J. E., Savitsky, P., Gileadi, O., von Delft, F., Rose, N. R., Offer, J., Scheinost, J. C., Borowski, T., Sundstrom, M., Schofield, C. J., and Oppermann, U. (2007) *Nature* **448,** 87–91
27. Yu, L., Wang, Y., Huang, S., Wang, J., Deng, Z., Zhang, Q., Wu, W., Zhang, X., Liu, Z., Gong, W., and Chen, Z. (2010) *Cell Res.* **20,** 166–173
28. Yue, W. W., Hozjan, V., Ge, W., Loenarz, C., Cooper, C. D., Schofield, C. J., Kavanagh, K. L., Oppermann, U., and McDonough, M. A. (2010) *FEBS Lett.* **584,** 825–830
29. Chen, Z., Zang, J., Kappler, J., Hong, X., Crawford, F., Wang, Q., Lan, F., Jiang, C., Whetstine, J., Dai, S., Hansen, K., Shi, Y., and Zhang, G. (2007) *Proc. Natl. Acad. Sci. U.S.A.* **104,** 10818–10823
30. Horton, J. R., Upadhyay, A. K., Qi, H. H., Zhang, X., Shi, Y., and Cheng, X. (2010) *Nat. Struct. Mol. Biol.* **17,** 38–43
31. Katoh, M., and Katoh, M. (2004) *Int. J. Oncol.* **24,** 1623–1628
32. Wissmann, M., Yin, N., Müller, J. M., Greschik, H., Fodor, B. D., Jenuwein, T., Vogler, C., Schneider, R., Günther, T., Buettner, R., Metzger, E., and Schüle, R. (2007) *Nat. Cell Biol.* **9,** 347–353
33. Katoh, Y., and Katoh, M. (2007) *Int. J. Mol. Med.* **20,** 269–273
34. Liu, G., Bollig-Fischer, A., Kreike, B., van de Vijver, M. J., Abrams, J., Ethier, S. P., and Yang, Z. Q. (2009) *Oncogene* **28,** 4491–4500
35. Strobl-Mazzulla, P. H., Sauka-Spengler, T., and Bronner-Fraser, M. (2010) *Dev. Cell* **19,** 460–468
36. Klose, R. J., Yamane, K., Bae, Y., Zhang, D., Erdjument-Bromage, H., Tempst, P., Wong, J., and Zhang, Y. (2006) *Nature* **442,** 312–316
37. Whetstine, J. R., Nottke, A., Lan, F., Huarte, M., Smolikov, S., Chen, Z., Spooner, E., Li, E., Zhang, G., Colaiacovo, M., and Shi, Y. (2006) *Cell* **125,** 467–481
38. Chen, Z., Zang, J., Whetstine, J., Hong, X., Davrazou, F., Kutateladze, T. G., Simpson, M., Mao, Q., Pan, C. H., Dai, S., Hagman, J., Hansen, K., Shi, Y., and Zhang, G. (2006) *Cell* **125,** 691–702
39. Shin, S., and Janknecht, R. (2007) *Biochem. Biophys. Res. Commun.* **359,** 742–746
40. Shin, S., and Janknecht, R. (2007) *Biochem. Biophys. Res. Commun.* **353,** 973–977
41. Rose, N. R., Ng, S. S., Mecinovi, J., Liénard, B. M., Bello, S. H., Sun, Z., McDonough, M. A., Oppermann, U., and Schofield, C. J. (2008) *J. Med. Chem.* **51,** 7053–7056
42. Rose, N. R., Woon, E. C., Kingham, G. L., King, O. N., Mecinovi, J., Clifton, I. J., Ng, S. S., Talib-Hardy, J., Oppermann, U., McDonough, M. A., and Schofield, C. J. (2010) *J. Med. Chem.* **53,** 1810–1818
43. King, O. N., Li, X. S., Sakurai, M., Kawamura, A., Rose, N. R., Ng, S. S., Quinn, A. M., Rai, G., Mott, B. T., Beswick, P., Klose, R. J., Oppermann, U., Jadhav, A., Heightman, T. D., Maloney, D. J., Schofield, C. J., and Simeonov, A. (2010) *PLoS One* **5,** e15535
44. Collaborative Computational Project No. 4 (1994) *Acta Crystallogr. D Biol. Crystallogr.* **50,** 760–763
45. McCoy, A. J., Grosse-Kunstleve, R. W., Storoni, L. C., and Read, R. J. (2005) *Acta Crystallogr. D Biol. Crystallogr.* **61,** 458–464
46. Perrakis, A., Morris, R., and Lamzin, V. S. (1999) *Nat. Struct. Biol.* **6,** 458–463
47. Murshudov, G. N., Vagin, A. A., and Dodson, E. J. (1997) *Acta Crystallogr. D Biol. Crystallogr.* **53,** 240–255
48. Emsley, P., and Cowtan, K. (2004) *Acta Crystallogr. D Biol. Crystallogr.* **60,** 2126–2132
49. Fodor, B. D., Kubicek, S., Yonezawa, M., O'Sullivan, R. J., Sengupta, R., Perez-Burgos, L., Opravil, S., Mechtler, K., Schotta, G., and Jenuwein, T. (2006) *Genes Dev.* **20,** 1557–1562
50. Wang, J., Zhang, M., Zhang, Y., Kou, Z., Han, Z., Chen, D. Y., Sun, Q. Y., and Gao, S. (2010) *Biol. Reprod.* **82,** 105–111
51. Loh, Y. H., Zhang, W., Chen, X., George, J., and Ng, H. H. (2007) *Genes Dev.* **21,** 2545–2557
52. Ishimura, A., Terashima, M., Kimura, H., Akagi, K., Suzuki, Y., Sugano, S., and Suzuki, T. (2009) *Biochem. Biophys. Res. Commun.* **389,** 366–371
53. Amores, A., Force, A., Yan, Y. L., Joly, L., Amemiya, C., Fritz, A., Ho, R. K., Langeland, J., Prince, V., Wang, Y. L., Westerfield, M., Ekker, M., and Postlethwait, J. H. (1998) *Science* **282,** 1711–1714
54. Klose, R. J., Gardner, K. E., Liang, G., Erdjument-Bromage, H., Tempst, P., and Zhang, Y. (2007) *Mol. Cell. Biol.* **27,** 3951–3961
55. Huang, Y., Fang, J., Bedford, M. T., Zhang, Y., and Xu, R. M. (2006) *Science* **312,** 748–751
56. Lee, J., Thompson, J. R., Botuyan, M. V., and Mer, G. (2008) *Nat. Struct. Mol. Biol.* **15,** 109–111
57. Ponnaluri, V. K., Vavilala, D. T., Putty, S., Gutheil, W. G., and Mukherji, M. (2009) *Biochem. Biophys. Res. Commun.* **390,** 280–284
58. Ponnaluri, V. K., Vavilala, D. T., and Mukherji, M. (2011) *Biochem. Biophys. Res. Commun.* **405,** 588–592
59. Azuara, V., Perry, P., Sauer, S., Spivakov, M., Jørgensen, H. F., John, R. M., Gouti, M., Casanova, M., Warnes, G., Merkenschlager, M., and Fisher, A. G. (2006) *Nat. Cell Biol.* **8,** 532–538
60. Bernstein, B. E., Mikkelsen, T. S., Xie, X., Kamal, M., Huebert, D. J., Cuff, J., Fry, B., Meissner, A., Wernig, M., Plath, K., Jaenisch, R., Wagschal, A., Feil,

R., Schreiber, S. L., and Lander, E. S. (2006) *Cell* **125,** 315–326
61. Leung, I. K., Krojer, T. J., Kochan, G. T., Henry, L., von Delft, F., Claridge, T. D., Oppermann, U., McDonough, M. A., and Schofield, C. J. (2010) *Chem. Biol.* **17,** 1316–1324
62. Ehrismann, D., Flashman, E., Genn, D. N., Mathioudakis, N., Hewitson, K. S., Ratcliffe, P. J., and Schofield, C. J. (2007) *Biochem. J.* **401,** 227–234
63. Kaelin, W. G., Jr., and Ratcliffe, P. J. (2008) *Mol. Cell* **30,** 393–402
64. Loenarz, C., Coleman, M. L., Boleininger, A., Schierwater, B., Holland, P. W., Ratcliffe, P. J., and Schofield, C. J. (2011) *EMBO Rep.* **12,** 63–70
65. Pollard, P. J., Loenarz, C., Mole, D. R., McDonough, M. A., Gleadle, J. M., Schofield, C. J., and Ratcliffe, P. J. (2008) *Biochem. J.* **416,** 387–394
66. Beyer, S., Kristensen, M. M., Jensen, K. S., Johansen, J. V., and Staller, P. (2008) *J. Biol. Chem.* **283,** 36542–36552
67. Krieg, A. J., Rankin, E. B., Chan, D., Razorenova, O., Fernandez, S., and Giaccia, A. J. (2010) *Mol. Cell. Biol.* **30,** 344–353
68. Yang, J., Jubb, A. M., Pike, L., Buffa, F. M., Turley, H., Baban, D., Leek, R., Gatter, K. C., Ragoussis, J., and Harris, A. L. (2010) *Cancer Res.* **70,** 6456–6466